



Research Article

Tetramethylpyrazine attenuates renal tubular epithelial cell ferroptosis in contrast-induced nephropathy by inhibiting transferrin receptor and intracellular reactive oxygen species

Zhongqiang Zhu^{1,2,*},  Jun Li^{1,*}, Zhiyong Song^{1,*}, Tonglu Li¹, Zongping Li¹ and  Xuezhong Gong¹

¹Department of Nephrology, Shanghai Municipal Hospital of Traditional Chinese Medicine, Shanghai University of Traditional Chinese Medicine, Shanghai, China; ²Shuguang Hospital Affiliated to Shanghai University of Traditional Chinese Medicine, Shanghai, China

Correspondence: Xuezhong Gong (shnanshan@yeah.net)



Contrast-induced nephropathy (CIN) is a leading cause of hospital-acquired acute kidney injury (AKI). Recently, ferroptosis was reported to be crucial for AKI pathogenesis. Our previous studies indicated antioxidant tetramethylpyrazine (TMP) prevent CIN *in vivo*. However, whether ferroptosis is involved in TMP nephroprotective mechanism against CIN is unclear. In the present study, we investigated the role of renal tubular epithelial cell ferroptosis in TMP reno-protective effect against CIN and the molecular mechanisms by which TMP regulates ferroptosis. Classical contrast-medium, iohexol, was used to construct CIN models in rats and HK-2 cells. Results showed that tubular cell injury was accompanied by ferroptosis both *in vivo* and *in vitro*, including the typical features of ferroptosis, Fe²⁺ accumulation, lipid peroxidation and decreased glutathione peroxidase 4 (GPX4). Ferroptosis inhibition by classic inhibitors Fer-1 and DFO promoted cell viability and reduced intracellular ROS production. Additionally, TMP significantly inhibited renal dysfunction, reduced AKI biomarkers, prevented ROS production, inhibited renal Fe²⁺ accumulation and increased GPX4 expression. Expressions of various proteins associated with iron ion metabolism, including transferrin receptor (TFRC), divalent metal transporter 1, iron-responsive element binding protein 2, ferritin heavy chain 1, ferroportin 1, and heat shock factor binding protein 1, were examined using mechanistic analyses. Among these, TFRC changes were the most significant after TMP pretreatment. Results of siRNA knockdown and plasmid overexpression of TFRC indicated that TFRC is essential for TMP to alleviate ferroptosis and reduce LDH release, Fe²⁺ accumulation and intracellular ROS. Our findings provide crucial insights about the potential of TMP in treating AKI associated with ferroptosis.

Introduction

Acute kidney injury (AKI) is a multifactorial group of clinical syndromes characterized by a rapid decline in renal function [1]. Available studies suggest that 10–15% of hospitalized patients are at risk of AKI, and the incidence may exceed 50% in intensive care unit [2,3]. Contrast-induced nephropathy (CIN), also known as contrast medium (CM)-induced AKI (CI-AKI), is an important component of hospital-acquired AKI [4]. Although multiple mechanisms, including inflammation, oxidative stress, and hemodynamics, have been reported in the pathogenesis of AKI, effective therapeutic interventions are lacking [5]. In 2012, Dixon et al. first reported ferroptosis, a type of iron-dependent non-apoptotic cell death. Ferroptosis involves the accumulation of iron and lipid peroxides, leading to oxidative stress and impairment of cellular membranes [6].

*These authors contributed equally to this work.

Received: 10 October 2023
Revised: 12 February 2024
Accepted: 14 February 2024

Accepted Manuscript online:
14 February 2024
Version of Record published:
27 February 2024

The regulation of ferroptosis is influenced by various factors, including iron metabolism, lipid peroxidation, and antioxidant systems. Ferroptosis is initiated by the accumulation of lipid peroxides generated from the oxidation of polyunsaturated fatty acids by lipoxygenases or other enzymes. The accumulation of lipid peroxides due to the oxidation of polyunsaturated fatty acids by lipoxygenases or other enzymes can trigger ferroptosis. Subsequently, lipid peroxide accumulation is amplified by the iron-catalyzed Fenton reaction, generating reactive oxygen species (ROS) and hydroxyl radicals that attack and damage cellular components, particularly cell membranes, leading to cell death [7]. As ferroptosis is a novel form of programmed cell death, recent studies have emphasized the role of ferroptosis in multiple AKI models, such as cisplatin, ischemia–reperfusion injury (IRI), and folic acid (FA), but not in CIN. In the AKI model of IRI, ferroptosis induces synchronized tubular necrosis, as observed using microscopy, whereas ferroptosis inhibitors exert potent nephroprotective effects under severe IRI conditions [8]. The acyl-CoA synthetase long-chain family (ACSL4) is a ferroptosis-promoting gene, and ACSL4 knockdown significantly reduced ferroptosis and alleviated renal inflammatory infiltration and pathological injury in IRI- and FA-induced AKI mice [9]. Various natural compounds inhibit AKI by targeting ferroptosis. Quercetin, a natural flavonoid, inhibits ferroptosis in renal proximal tubular epithelial cells in an AKI model as well as ferroptosis-induced macrophage chemotaxis [10]. Additionally, ginsenoside Rg1 attenuates AKI in septic rats by inhibiting ferroptosis in renal tubular epithelial cells via ferroptosis suppressor protein 1 (FSP1) [11]. Therefore, the modulation of ferroptosis in AKI is a promising target for alleviating renal injury.

Tetramethylpyrazine (TMP) is a bioactive component contained in traditional Chinese medicine Chuanxiong (*Ligusticum chuanxiong* Hort), with nephroprotective effects because of its antioxidant activity [12]. Over the years of exploration, our team has proven that TMP can attenuate renal damage in a CIN animal model through multiple pathways, of which the regulation of tubular epithelial cell death is the most important. In CIN model rats, TMP significantly attenuated renal tubular cell apoptosis, possibly by inhibiting the p38 MAPK and FoxO1 pathways [13]. In another study, we demonstrated that TMP inhibited the activation of the CCL2/CCR2 pathway in CIN, ameliorated renal oxidative stress and abnormal mitochondrial dynamics, and modulated mitochondrial autophagy in renal tubular cells [14]. However, whether ferroptosis is involved in the nephroprotective effects of TMP against CIN remains unclear. In the present study, we explored the potential mechanisms by which TMP regulates ferroptosis in CIN.

Materials and methods

Reagents

All chemicals were purchased from Sigma (St. Louis, Mo., U.S.A.) unless otherwise stated. The iodinated radiographic contrast agent used in this study was iohexol (Omnipaque 300 mg I/ml) and was purchased from Amersham Health (Princeton, N.J., U.S.A.).

Animal and experiment design

A total of 24 adult 8- to 10-week-old male Sprague-Dawley rats weighing 200–250 g were purchased from the Shanghai Lab Animal Research Center. The rats were housed in an air-conditioned room at 23°C with a 12/12 h light/dark cycle. Food and water were provided ad libitum, except on the dehydration day. We used a well-established animal model of CIN [13]. Twenty-four rats were randomly divided into three groups of eight rats each ($n=8$): control (Con), rats injected with iohexol (CIN), and rats injected with iohexol and treated with TMP (CIN + TMP). On days 1–4, rats in the CIN + TMP group were intraperitoneally (i. p.) administered 80 mg/kg TMP once daily, whereas rats in the Con and CIN groups were administered an equivalent volume of saline. All rats were dehydrated for 24 h on day 3. On day 4, after 20 min of saline or TMP injection, rats were injected with a nitric oxide synthase inhibitor (NG-nitro-L-arginine methyl ester, L-NAME, 10 mg/kg, i.p.), followed by injection of an inhibitor of prostaglandin synthesis (indomethacin, 10 mg/kg, i.p.) and iohexol (1.5–2 g iodine/kg, i.p.) after 15 and 30 min, respectively, to a construct CIN rat model. The Con group was administered an equivalent volume of saline. Animals were killed 24 h after modeling under terminal general isoflurane anesthesia. Serum was obtained from the blood collected from the tail vein, and kidneys were collected for biochemical and morphological examinations. The urinary N-acetyl- β -glucosaminidase (UNAG) and urinary γ -glutamyl transpeptidase (UGGT) analyses in 24-h urine samples were conducted on the same day. A flowchart of the CIN animal model construction is shown in Figure 1A. The present study was approved by the Medicine Animal Ethics Committee of Shanghai Municipal Hospital of Traditional Chinese Medicine (No. 2020025), and animal experiments were conducted in the animal room of Shanghai Municipal Hospital of Traditional Chinese Medicine.

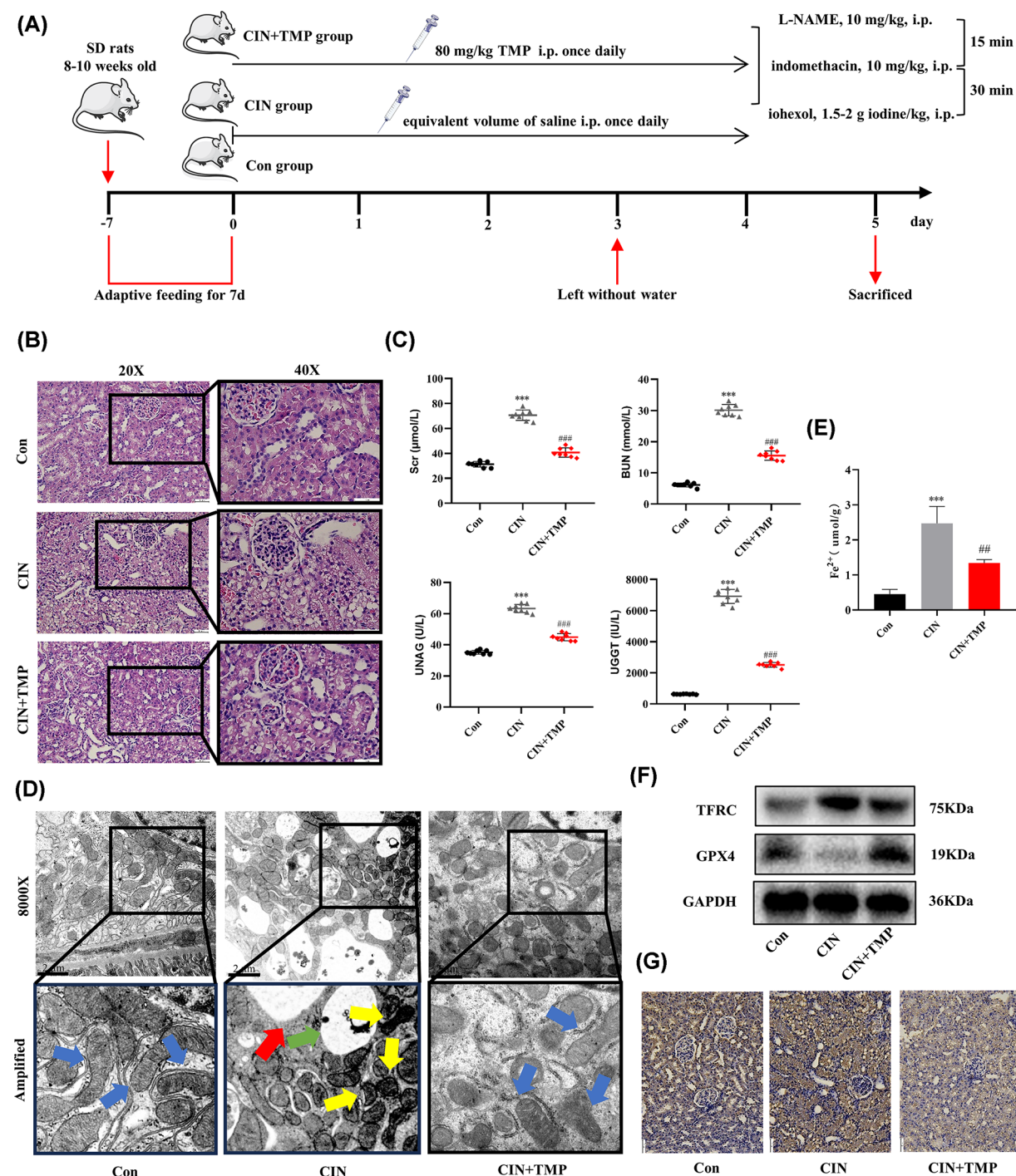


Figure 1. TMP alleviated kidney injury and ferroptosis in rats with CIN

(A) Flowchart of CIN rat model construction. **(B)** Hematoxylin-eosin staining of renal tissue. **(C)** Scr, BUN, UNAG, and UGGT levels of rats with CIN ($n = 8$). **(D)** Representative images of ferroptosis in kidney tissue based on transmission electron microscopy (8000 \times). The blue arrow indicates normal mitochondria, yellow arrow indicates smaller mitochondria with the increased membrane density, whereas the mitochondrial cristae decreased in size or disappeared, suggesting the occurrence of ferroptosis, red arrow indicates mitochondrial edema and vacuolar degeneration, and green arrow indicates autophagic vacuole. **(E)** Detection of Fe^{2+} content in renal tissue. **(F)** Western blotting results of TFRC and GPX4. **(G)** Immunohistochemistry of TFRC in renal tissues of rats with CIN. Data were representative images or were expressed as the mean \pm SD of $n = 3$ experiments. Notes: *** $P < 0.001$ vs. control group. ## $P < 0.01$ vs. iohexol treatment. #### $P < 0.001$ vs. iohexol treatment.

Cell cultures and treatments

A classic CIN cell model was established using iohexol in HK-2 cells *in vitro* [15]. HK-2 cells were cultured in DMEM/F12 medium containing 10% FBS and placed in a cell culture incubator at 37°C and 5% CO₂. When the cells reached 80% confluence, cell passages were performed, and the 6–12 generation cells were used for subsequent experiments. Cells in a good logarithmic growth phase were incubated with iohexol (75 mgI/ml) in the presence or absence of TMP (100 and 200 µM), iron chelator deferoxamine mesylate (DFO, 30 µM), and ferroptosis inhibitor ferrostatin-1 (Fer-1, 3 µM). Cells in vehicle control group were cultured under normal conditions with an equal volume of PBS as above treatment. Cell activity was assessed at each time point using the cell counting kit-8 (CCK-8) assay.

Cell transfection

HK2 cells were seeded in 24-well plates at 1×10^5 cells/well, and the complete medium was replaced with serum-free medium before transfection. Using the Lipofectamine™ 2000 liposome method, transferrin receptor (TFRC) siRNA sequences (si-TFRC1, si-TFRC2, and si-TFRC3), control sequences (si-NC), empty vector plasmid (vector), and TFRC overexpression plasmid (oeTFRC) were transfected. Furthermore, the knockdown and overexpression of TFRC were verified using quantitative real-time polymerase chain reaction (qRT-PCR) and Western blotting. The cells were collected for the subsequent two parts of the experiment, which were performed as described above. First, we studied the effects of siRNA and TFRC overexpression on cell viability and ferroptosis in 75 mgI/ml iohexol-treated HK-2 cells. Second, we confirmed whether TFRC overexpression affected the anti-ferroptotic and cytoprotective effects of TMP in CIN HK-2 cells.

Hematoxylin–eosin (HE) staining

The harvested kidney tissues were fixed in 4% paraformaldehyde, embedded in paraffin, cut into 5-µm sections, and preheated in an oven at 60°C for 8–10 min. Xylene, anhydrous ethanol, 95% ethanol, and 85% ethanol were sequentially used for dewaxing. The sections were stained in hematoxylin and eosin solutions for 3–5 and 2 min, respectively. Ethanol (95%) and anhydrous ethanol were sequentially used for dehydration. The neutral gum was used for sealing after xylene permeate treatment, and histomorphological changes were observed under the microscope (DM6B, Leica, Germany).

Immunohistochemical (IHC) staining

Kidney tissues were fixed in 4% paraformaldehyde, embedded in paraffin, and cut into 5-µm sections. Antigen retrieval was performed using trypsin at 37°C. The prepared tissue sections were incubated overnight at 4°C with primary antibodies against TFRC (1:1000, ab214039, Abcam). Subsequently, the secondary antibodies (PV-9001, ZSGB-BIO, China) were incubated separately at 37°C for 20 min. After DAB color development, the hematoxylin solution was used for staining for 2–3 min. Ethanol (95%) and anhydrous ethanol were sequentially used for dehydration. The neutral gel was used for sealing after xylene permeation treatment, and the results were observed under a microscope (DM6B, Leica, Germany).

Transmission electron microscopy (TEM)

Collected renal cortex tissues were fixed using 1% osmic acid in 0.1 M PBS (pH 7.4). Then, the specimens were stained with lead rafter acid in 2% uranium acetate saturated aqueous solution. After being washed with PBS and dehydrated with acetone, the specimens were subsequently embedded in epoxy resin. Finally, transmission electron micrographs were prepared using a transmission electron microscope (JEOLUSA, Inc., Peabody, MA, U.S.A.) to observe the cellular ultrastructure.

Morphology

Morphological changes were routinely checked under phase contrast microscope. To compare the concentration-dependent and time-dependent effects of TMP on iohexol-induced cellular damage, a range of TMP concentrations (100 and 200 µM) and exposure times (0, 3, 6, 12 and 24 h) were examined.

CCK-8 assay for cell viability

Well-grown HK-2 cells were inoculated into 100 µl of growth medium in 96-well plates. At 0, 3, 6, 12, and 24 h after treatment, 10 µl of CCK-8 working solution was added to each well in each group. After incubation at 37°C for 2 h, the absorbance of each well was measured at 450 nm using an enzyme labeler.

Table 1 Gene primer sequences

Gene (Human)	Primer	Sequence
TFRC	Forward	ATGGCGATAACAGTCATGTGGA
	Reverse	CCAATATAAGCGACGTGCTGC
DMT1	Forward	AGCTGTCATCATGCCACACA
	Reverse	AGACTTCAACCACCTGCTCG
IREB2	Forward	GGAAACTCCAGAGACTGGGC
	Reverse	GAGGCCCAAGGAATCTGCAT
FTH1	Forward	ACGCCTCCTACGTTTACCTG
	Reverse	GAAGATTTCGGCCACCTCGTT
FPN1	Forward	ATCCTTGGCCGACTACCTGA
	Reverse	CCAGTCACCGATGATGGCTC
HSBP1	Forward	GAGACTGACCCCAAGACCGT
	Reverse	ACTCTTTTTCGCTGGCAGGTA

qRT-PCR

Total RNA was extracted from HK-2 cells using the TRIzol method, and RNA concentration and purity were determined. The cDNA was prepared using the cDNA reverse transcription kit. Three replicate wells were set up for each sample, and the relative expression of TFRC, divalent metal transporter 1 (DMT1), iron-responsive element binding protein 2 (IREB2), FTH1, ferroportin 1 (FPN1), and heat shock factor binding protein 1 (HSBP1) was calculated using the $2^{-\Delta\Delta C_t}$ method. β -Actin was used as the internal reference. The primer sequences are listed in Table 1.

Western blotting

Western blotting was performed as described previously [16,17]. The primary antibodies used were anti-TFRC (1:1000, ab214039, Abcam), anti-GPX4 (1:1000, ab125066, Abcam), and anti-GAPDH (1:1000, Cell Signaling Technology). All experiments were performed at least three times ($n=3$) under the same conditions.

Detection lipid ROS, intracellular Fe^{2+} , LDH and GSH

Intracellular ROS levels were measured using BODIPY 581/591 C11 (Invitrogen, D3861). The treated cells were thoroughly washed with PBS twice before being digested with trypsin. Following centrifugation at 1000 rpm for 5 min, the cell precipitate was carefully collected. The cells were then resuspended in 1 ml of PBS. To create the probe staining working solution, the BODIPYTM probe was diluted in serum-free medium to achieve a concentration of 2 μM . For each experimental group, the cell suspension was centrifuged at 1000 rpm for 5 min. The supernatant was then discarded, and the cells were resuspended using the probe staining working solution. The cells were incubated at a concentration of 1,000,000/ml for 30 min at 37°C, protected from light, and stirred every 3–5 min to ensure complete contact between the probe and the cells. After the incubation period, the cells were washed three times with serum-free medium to thoroughly remove any BODIPYTM that had not been internalized. ROS-positive cells exhibited a strong green fluorescence, which was detected in real-time using flow cytometry. Intrarenal and intracellular ferrous ion, LDH and GSH concentrations were detected by Ferrous Ion Content Assay Kit (Solarbio, BC5415), LDH activity assay kit (Solarbio, BC0685), and Reduced Glutathione (GSH) Content Assay Kit (Solarbio, BC1175) on snap-frozen kidney tissue or the collected cells following the manufacturer's instructions.

Statistical analysis

GraphPad Prism software was used to statistically analyze the data, and the measurement data satisfying normal distribution and chi-square were expressed as mean \pm SD. One-way ANOVA was used for comparison between multiple groups, and t -test was used for comparison between two groups. The test level (α) was 0.05.

Results

TMP preserved renal function in rats with CIN

To investigate the effects of TMP on renal tubular injury in rats with CIN, we injected SD rats with iohexol to induce AKI. Histological analysis demonstrated the protective effect of TMP against renal tubular injury. Compared with the Con group, renal tubular mesenchymal injury in the CIN group was severe, including apparent swelling and vacuolization of renal tubular epithelial cells, whereas the glomeruli were unaffected. After TMP treatment, the

symptoms of tissue injury were significantly alleviated (Figure 1B). As shown in Figure 1C, TMP treatment significantly reduced serum creatinine and blood urea nitrogen levels ($P < 0.001$). In addition, pre-administration of TMP reduced the expression of AKI biomarkers, including UNAG and UGGT, in urine ($P < 0.001$).

TMP alleviated ferroptosis and Fe^{2+} accumulation in rats with CIN

Ferroptosis is a regulated cellular necrosis caused by iron ion-catalyzed and ROS-induced lipid peroxidation. Therefore, we focused on oxidative stress-related indicators and ferrous ions. Oxidative stress is an important driving mechanism of CIN and is the pathological basis of antioxidant therapy for CIN [18]. In previous studies, we demonstrated the involvement of ROS in localized renal injury in a CIN model, indicated by a dramatic decrease in SOD and GSH and an increase in MDA in renal tissues [19]. Therefore, we hypothesize that the alleviation of CIN renal injury by TMP is accompanied by an attenuation of lipid peroxidation. Mitochondrial alterations are an important feature of ferroptosis. An ultrastructural examination showed smaller mitochondria, increased membrane density, and reduced mitochondrial cristae in the kidney tissues of rats with CIN, which exhibited typical features of ferroptosis. Moreover, TMP alleviated mitochondrial abnormalities (Figure 1D). Localized iron-ion levels have also been examined as a distinguishing feature of ferroptosis. The ferrous ion content assay showed that Fe^{2+} accumulation in the renal tissue was significantly higher in the CIN group, which suggested the possibility of localized iron overload, whereas TMP significantly alleviated this process (Figure 1E).

Moreover, we also monitored the levels of key signaling proteins, TFRC and GPX4, during ferroptosis. The results revealed a significant up-regulation of TFRC expression in the CIN group, whereas TMP treatment effectively reversed this trend (Figure 1F). In contrast with TFRC, the expression level of GPX4 was noticeably down-regulated in the CIN group. However, TMP treatment reversed this trend and significantly up-regulated GPX4 expression. For immunohistochemical analysis, we used anti-TFRC antibodies, which revealed that TMP treatment led to a reduction in TFRC expression compared with the CIN group (Figure 1G).

TMP alleviated cell death, Fe^{2+} accumulation, and ferroptosis *in vitro*

We first verified the protective effects of TMP against cell injury in a CIN cell model. Microscopically, this was accompanied by cell shrinkage, membrane blebbing, and brightly rounded bodies, indicating cell death after iohexol exposure (Figure 2A). Simultaneously, TMP pretreatment alleviated cell death induced by iohexol. To further investigate the dose–effect relationship of TMP, we used two concentrations of TMP, 100 and 200 μM , in subsequent studies. As shown in Figure 2B, cell viability was significantly reduced 6 h after iohexol exposure compared with the control group ($P < 0.001$). Compared with the iohexol group, 200 μM TMP treatment significantly promoted cell viability ($P < 0.001$). Notably, TMP performed better in promoting cell survival and was most effective at 24 h. Based on the cytoprotective effects of TMP, we explored its role on intracellular Fe^{2+} accumulation.

The results showed that the intracellular Fe^{2+} concentration increased after treatment with iohexol, while pretreatment with TMP significantly alleviated intracellular iron overload, with 200 μM TMP showing the best performance (Figure 2C). The hallmark of ferroptosis is the rupture of the cell membrane, resulting in the leakage of cytoplasmic contents into the culture medium, including LDH which has comparatively stable enzyme activity [20]. The results showed that TMP significantly alleviated LDH elevation and in iohexol-treated HK-2 cells ($P < 0.001$) (Figure 2D). Flow cytometry results showed that intracellular ROS production was significantly elevated in the iohexol group, whereas TMP pretreatment significantly inhibited this process ($P < 0.001$) (Figure 2E). To delve into the potential mechanism behind TMP's regulation of ferroptosis in CIN, we utilized qRT-PCR to further examine the expression levels of proteins involved in iron ion transport within cells. Compared with the control group, TFRC, DMT1, IREB2, and FPN1 were up-regulated and FTH1 and HSBP1 were down-regulated after iohexol exposure ($P < 0.05$) (Figure 2F). Notably, the change in TFRC was most significant after TMP pretreatment, especially in the 200 μM TMP group ($P < 0.001$ vs. iohexol group), which was also consistent with Western blotting results ($P < 0.001$) (Figure 2G).

Inhibition of ferroptosis promoted cell viability and reduced intracellular ROS production *in vitro*

To further verify the specific role of ferroptosis, HK-2 cells were treated with two classical ferroptosis inhibitors, Fer-1 and DFO, in the CIN cell model [21] (Figure 3A,B). Fer-1 is a synthetic antioxidant that prevents membrane lipid damage through a reduction mechanism, thereby inhibiting cell death during ferroptosis. DFO is an iron chelator that is commonly believed to inhibit intracellular iron overload during ferroptosis. Similar to TMP, Fer-1 and DFO treatment both achieved good performance in promoting cell viability and reducing intracellular ROS (Figure 3C,D). As shown in Figure 3C, cell viability was significantly reduced after iohexol exposure compared with the control

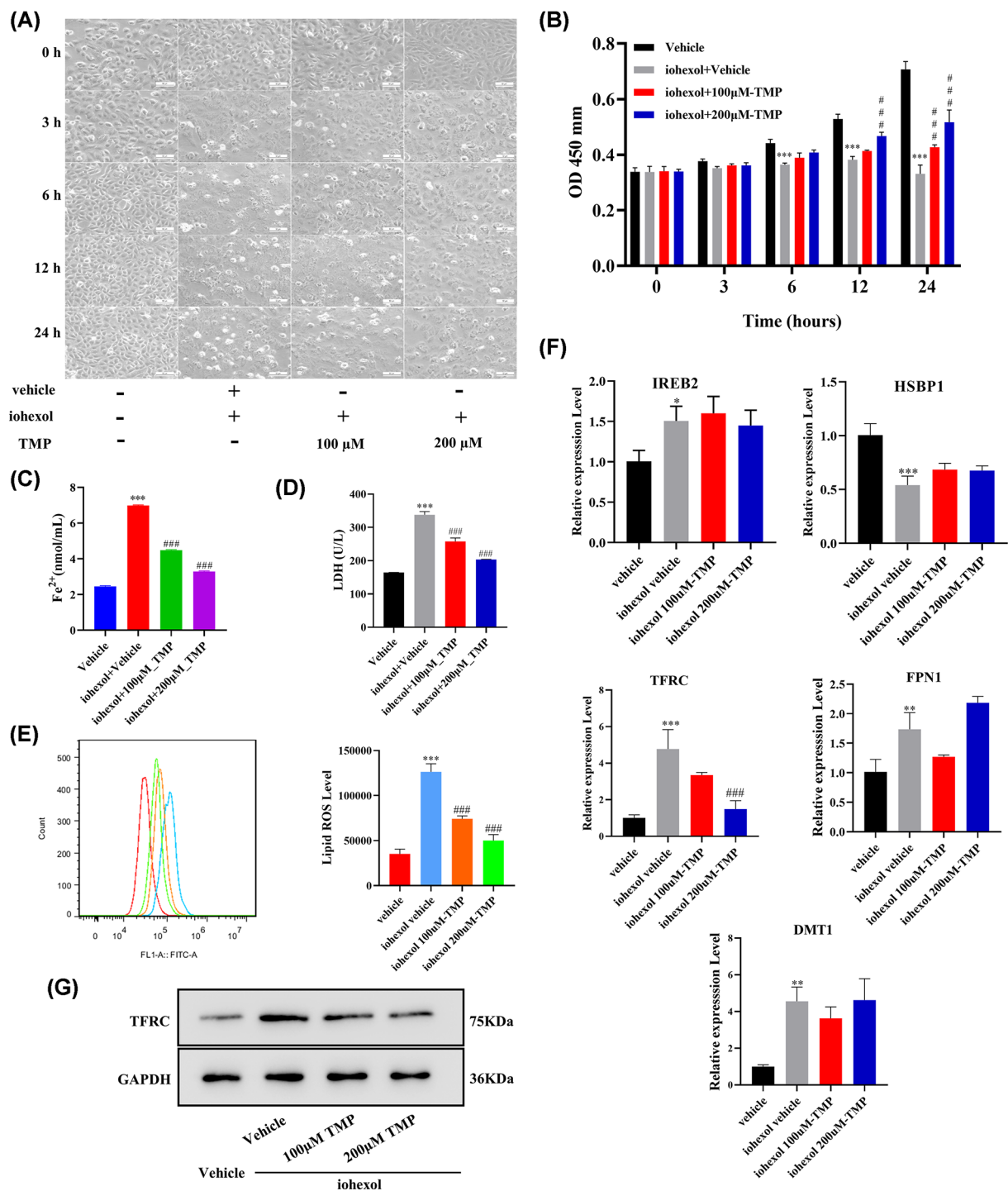


Figure 2. TMP alleviated intracellular Fe^{2+} accumulation and ferroptosis in CIN HK-2 cells

(A) Morphology was examined using phase-contrast microscopy at 200 \times magnification. (B) Cell viability was measured at 0, 3, 6, 12, and 24 h using CCK-8 assay. (C,D) Intracellular Fe^{2+} and LDH levels. (E) Intracellular ROS measured using flow cytometry. (F) qRT-PCR results of TFRC, DMT1, IREB2, FTH1, FPN1, and HSBP1. (G) Western blotting results of TFRC protein. Data were representative images or were expressed as the mean \pm SD of $n = 3$ experiments. Notes: * $P < 0.05$ vs. control group. ** $P < 0.01$ vs. control group. *** $P < 0.001$ vs. control group. # $P < 0.05$ vs. iohexol treatment. ### $P < 0.001$ vs. iohexol treatment.

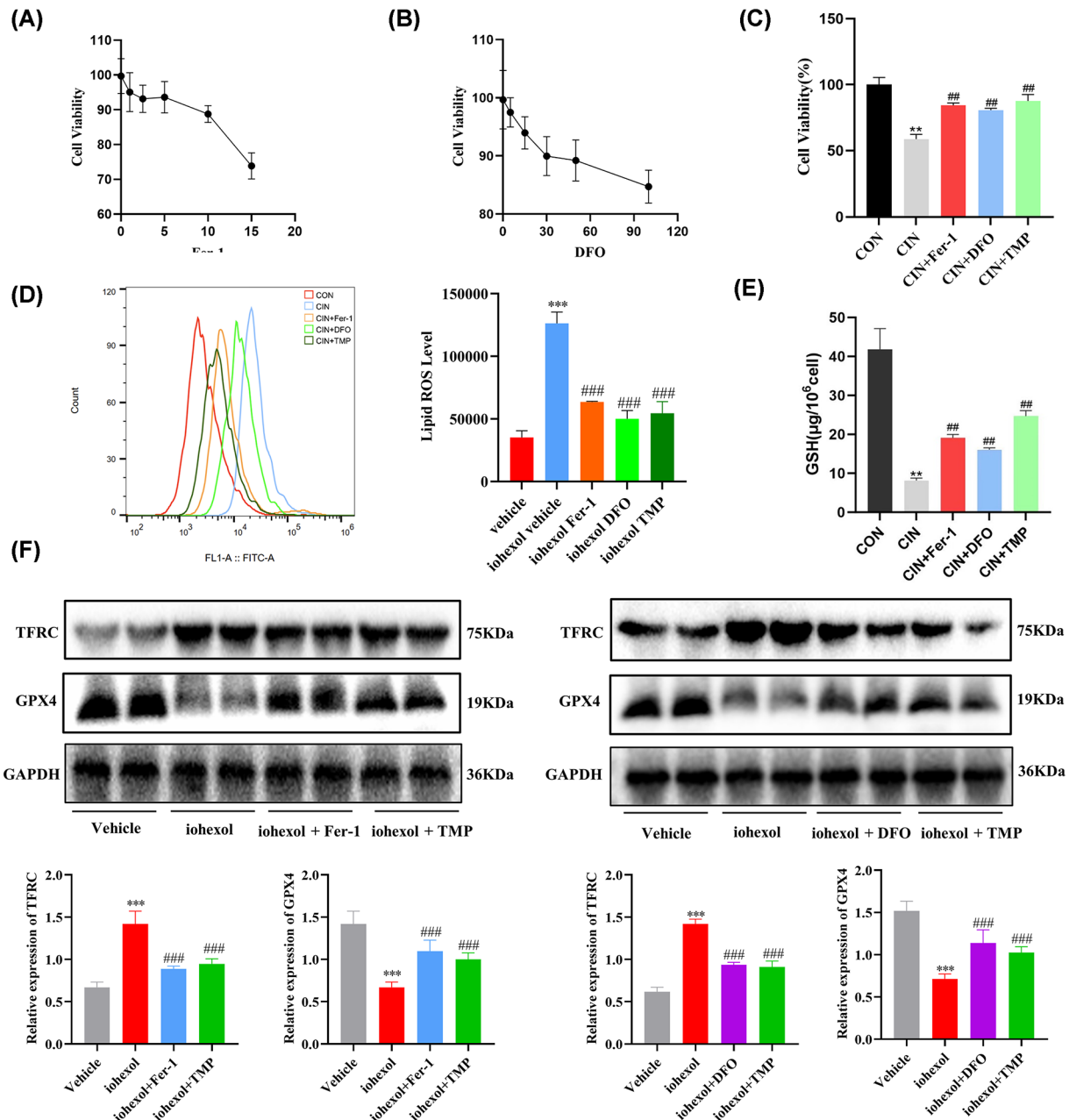


Figure 3. Ferroptosis inhibitors alleviated iohexol-induced cell death and intracellular ROS production *in vitro*

(A–C) HK-2 cell viability was tested by the CCK-8 assay after Fer-1 and DFO treatment. (D) Intracellular ROS measured using flow cytometry. (E) Detection of GSH level. (F) Western blotting results of GPX4 and TFRC. Data were representative images or were expressed as the mean \pm SD of $n = 3$ experiments. Notes: ** $P < 0.01$ vs. Vehicle group. *** $P < 0.001$ vs. Vehicle group. ## $P < 0.01$ vs. iohexol treatment. ### $P < 0.001$ vs. iohexol treatment.

group ($P < 0.001$). Compared with the iohexol group, both Fer-1 and DFO treatment significantly promoted cell viability ($P < 0.001$). This further validates the results of the *in vivo* study, which showed that inhibiting ferroptosis is beneficial for alleviating renal injury in CIN models. The results of lipid peroxidation levels detected by flow cytometry confirmed that Fer-1 and DFO significantly reduced the increase in intracellular ROS levels caused by iohexol (Figure 3D). Meanwhile, we observed a reduction in GSH levels in the model group, consistent with previous research findings, indicating an increase in lipid peroxidation, and ferroptosis inhibitors and TMP significantly mitigated the above process (Figure 3E). A significant body of research has established that GPX4 and TFRC, serves as a valuable

indicator for assessing ferroptosis in cells. After exposure to iohexol, the expression of GPX4 and TFRC proteins in HK-2 cells was either boosted or diminished. The application of Fer-1 and DFO, however, reversed this trend significantly, indicating the suppression of ferroptosis (Figure 3F). The above findings suggest that suppressing ferroptosis can mitigate intracellular ROS production and cell damage in CIN cell model. Additionally, TMP may possess the potential to inhibit ferroptosis in CIN.

TMP improved intracellular ROS production and ferroptosis in CIN by inhibiting TFRC

As described above, preliminary *in vitro* experiments suggested that TFRC may be a key target of TMP in regulating ferroptosis in CIN. To further clarify the critical role of TFRC in mediating ferroptosis in the CIN model, we knocked down TFRC in HK-2 cells through RNA interference. HK-2 cells were transfected with siRNA to inhibit TFRC expression (Figure 4A,B). Among the three siRNAs, siTFRC-1 and siTFRC-2 exhibited the highest interference efficiency and were selected for subsequent experiments. TFRC protein expression was up-regulated in CIN HK-2 cells, and siRNA interference reversed this trend (Figure 4C). As shown in Figure 4D, cell viability in the iohexol + siNC group significantly decreased from the 6th hour compared with that in the control group, whereas both siTFRC-1 and siTFRC-2 attenuated iohexol-induced cell damage ($P < 0.001$). si-TFRC also effectively alleviated LDH production, Fe^{2+} accumulation, and intracellular ROS production ($P < 0.001$) (Figure 4E–G). The above results robustly support the notion that TFRC plays a pivotal role in the pathogenesis of renal injury in CIN.

TFRC overexpression abolished the effects of TMP on ferroptosis and intracellular ROS production

To obtain further evidence that TMP regulates TFRC to alleviate ferroptosis in CIN, plasmid transfection was used to overexpress TFRC in HK-2 cells. TFRC protein and mRNA expression were significantly increased in the overexpression plasmid group compared to the empty vector plasmid and control groups ($P < 0.001$) (Figure 5A,B). Although TMP inhibited the iohexol-induced up-regulation of TFRC protein, transfection with the overexpression plasmid restored TFRC expression levels (Figure 5C). As shown in Figure 5D, 200 μM TMP alleviated iohexol-induced cell damage, whereas oeTFRC significantly reversed the nephroprotective effect of TMP ($P < 0.001$). Follow-up results further confirmed that overexpression of TFRC by oeTFRC aggregated cell damage and ferroptosis and down-regulated the nephroprotective effect of TMP. The inhibitory effects of TMP on LDH and intracellular Fe^{2+} in CIN HK-2 cells were reversed by oeTFRC ($P < 0.001$) (Figure 5E,F). Similarly, TMP effectively reverses intracellular ROS production triggered by iohexol, yet upon transfection with oeTFRC, this protective action is significantly diminished ($P < 0.001$) (Figure 5G). The comprehensive findings presented above robustly support the notion that TFRC plays a pivotal role in enabling TMP to mitigate ferroptosis and renal injury in CIN.

Discussion

Ferroptosis is a caspase-independent regulated cell death characterized by the accumulation of lipid ROS produced through iron-dependent lipid peroxidation [22]. An imbalance between oxidative stress and the antioxidant system plays a critical role in ferroptosis. In various animal models of AKI, the renal protective effects of iron chelators and inhibitors of ferroptosis have been initially demonstrated [23]. Specifically, in cases of folic acid-induced AKI, the ferroptosis inhibitor Fer-1 has been shown to effectively mitigate oxidative stress and prevent renal tubular cell death. These findings suggest that targeting ferroptosis could represent a promising therapeutic strategy for the treatment of AKI [24]. In a mouse model of rhabdomyolysis-induced AKI, Fer-1 has been observed to prevent cell death by inhibiting lipid peroxidation [25]. Furthermore, Fer-1 and DFO have been shown to effectively alleviate patulin-induced AKI in mice by inhibiting autophagy-dependent ferroptosis [26]. Our study has further confirmed *in vitro* that Fer-1 and DFO effectively mitigate renal tubular cell injury in CIN by curbing iron overload and lipid peroxidation. These findings indicate that targeting ferroptosis holds significant promise as a potential therapeutic approach for the treatment of AKI. Correspondingly, the current study confirms that TMP exhibits good therapeutic effects on renal injury in CI-AKI rat and cell models, and definitely regulates ferroptosis in renal tubular epithelial cells, thus our data also provide new laboratory evidence for the prevention and treatment of CI-AKI with TMP, and suggests that TMP is a regulator of ferroptosis.

As a clinical drug, TMP is widely used in treating myocardial infarction, cerebral infarction, and diabetic nephropathy in China [27]. The nephroprotective effects of TMP may be mediated mainly by the regulation of oxidative stress, tubular epithelial cell death, and inflammatory damage [28–31]. Numerous studies have shown that oxidative stress plays a key role in the development of CIN. Notably, contrast medium can cause intrarenal vasoconstriction and

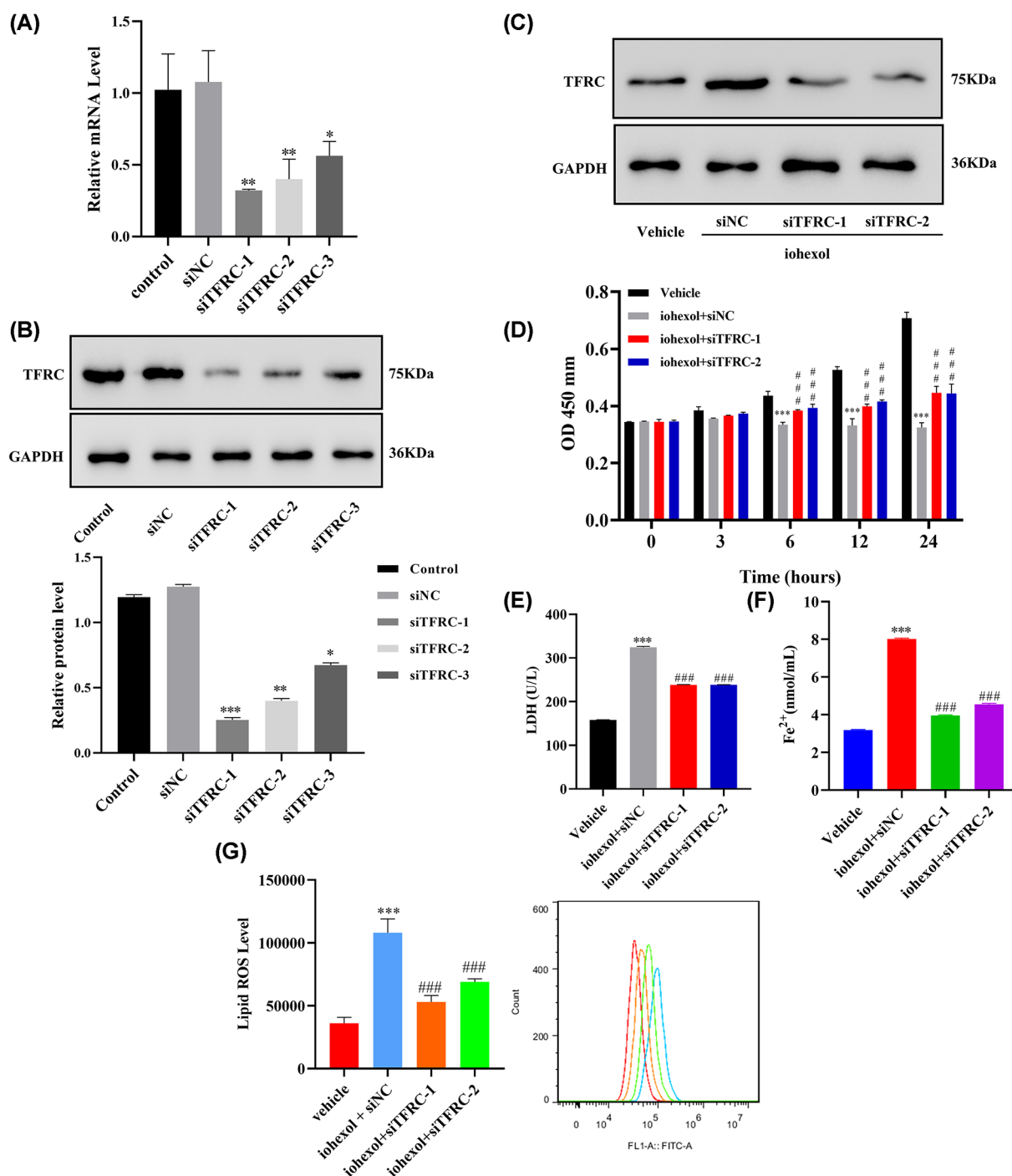


Figure 4. TMP alleviates ferroptosis in CIN by inhibiting TFRC

(A,B) The knockdown efficiency of TFRC in HK-2 cells was evaluated using qRT-PCR and Western blotting. (C) Western blotting results of TFRC protein in CIN HK-2 cells. (D) Cell viability was measured at 0, 3, 6, 12, and 24 h using CCK-8 assay. (E,F) LDH and intracellular Fe²⁺ levels. (G) Intracellular ROS measured using flow cytometry. Data were representative images or were expressed as the mean \pm SD of $n = 3$ experiments. Notes: ** $P < 0.01$ vs. control group. *** $P < 0.001$ vs. control group. # $P < 0.05$ vs. iohexol + siNC treatment. ## $P < 0.01$ vs. iohexol + siNC treatment. ### $P < 0.001$ vs. iohexol + siNC treatment.

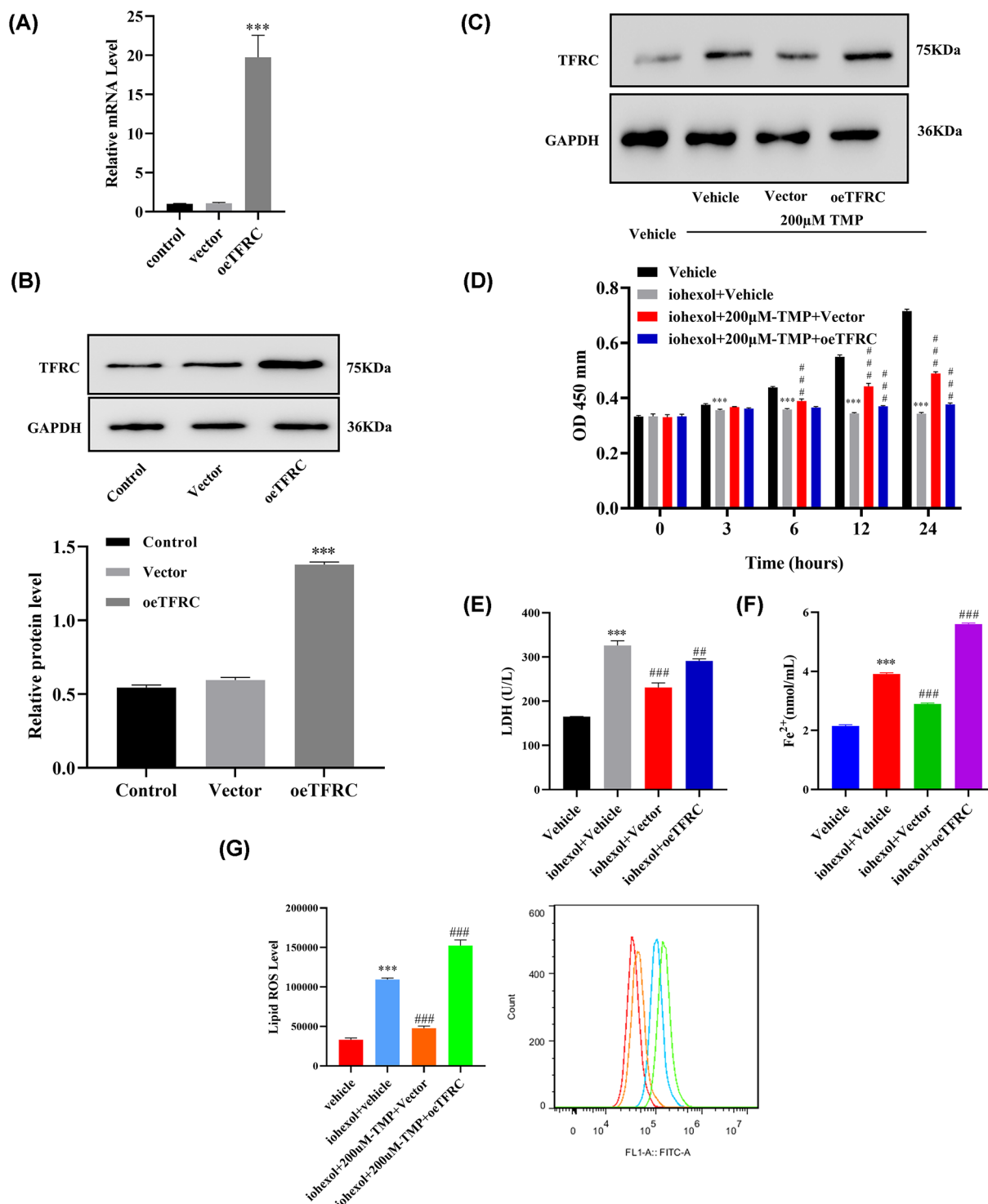


Figure 5. TFRC overexpression abolished the effects of TMP on ferroptosis and intracellular ROS production in CIN HK-2 cells

(A,B) The overexpression efficiency of TFRC in HK-2 cells was evaluated using qRT-PCR and Western blotting. (C) Western blotting results of TFRC protein. (D) Cell viability was measured at 0, 3, 6, 12, and 24 h using the CCK-8 assay. (E,F) LDH and intracellular Fe²⁺ levels. (G) Intracellular ROS measured using flow cytometry. Data were representative images or were expressed as the mean \pm SD of $n = 3$ experiments. Notes: * $P < 0.05$ vs. control group. ** $P < 0.01$ vs. control group. *** $P < 0.001$ vs. control group. # $P < 0.05$ vs. iohexol + vehicle. ### $P < 0.01$ vs. iohexol + vehicle. ### $P < 0.001$ vs. iohexol + vehicle.

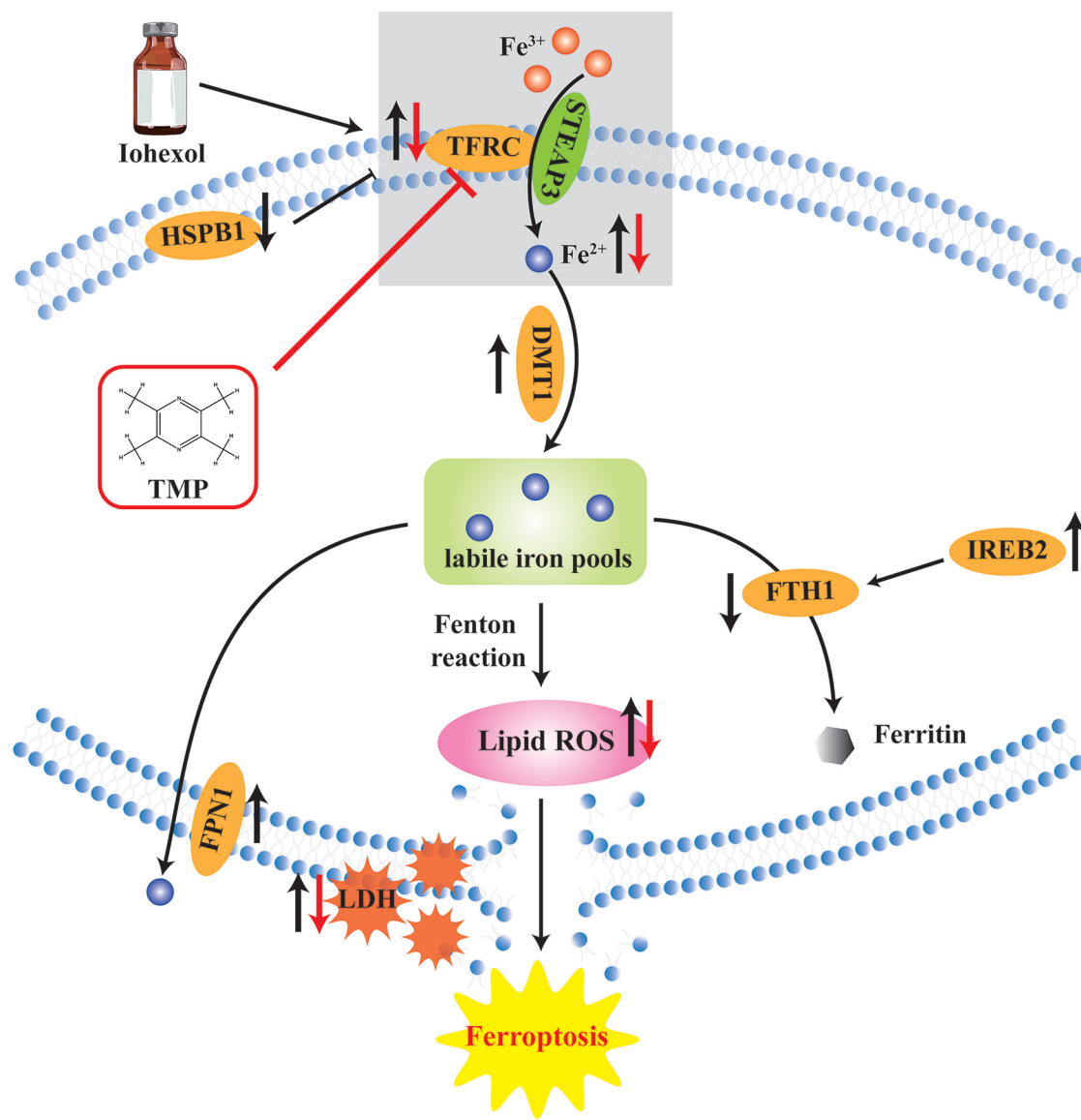


Figure 6. Mechanisms by which TMP modulates ferroptosis in CIN

After co-incubation with iohexol, various proteins associated with iron ion transport significantly changed, along with an upregulation of intracellular iron overload and lipid peroxidation (black arrows). After TMP pretreatment, only TFRC expression was reversed, which was accompanied by a down-regulation of intracellular Fe^{2+} and lipid peroxidation levels, suggesting that iohexol-induced ferroptosis was inhibited (red arrows). Therefore, TFRC-mediated ferroptosis plays crucial role in CIN. Antioxidant TMP could exert anti-ferroptosis effect by inhibiting TFRC expression and intracellular ROS production.

medullary hypoxia accompanied by excessive ROS production or reduced antioxidant enzyme activity [32]. In the present study, we used the FACS method to detect changes in ROS production in CIN rat and cell models. The results once again confirmed that the use of contrast medium induced a significant increase in ROS generation, accompanied by a decrease in the lipid peroxidation related indicator GSH. However, after the use of TMP, the above lesions were significantly reversed, which once again confirmed that TMP has good antioxidant and inhibitory effects on lipid peroxidation damage, consistent with our previous work [13,14,16,17].

Based on the present data, we also confirmed that ferroptosis of renal tubular epithelial cells does play an important role in CIN lesions. After CM exposure, ferroptosis of renal tubular epithelial cells significantly increased. After the use of ferroptosis specific inhibitors, Fer-1 and DFO, ferroptosis was significantly reduced, accompanied by an increase

in cell survival rate and a decrease in ROS generation (Figures 1–3). Interestingly, the ferroptosis induced by CM exposure was significantly inhibited after TM pretreatment, and the renal damages caused by CM in both *in vivo* and *in vitro* models were significantly reduced, the generations of ROS were reduced, and the reduced GSH levels were also significantly increased. These data confirm that TMP could have a certain regulatory effect on ferroptosis in renal tubular epithelial cells induced by oxidative stress and lipid peroxidation damage, which is clearly inseparable from its antioxidant effect.

In addition, we elucidated the regulatory mechanisms of TMP in regulating CM-induced renal tubular epithelial cell ferroptosis this process. In the *in vitro* experiments, we combined gene disruption and overexpression analyses to confirm that TFRC is critical for the regulation of ferroptosis by TMP in CIN. As shown in Figure 2, iron ion transport proteins, including TFRC, HSPB1, FPN1, DMT1, IREB2, and FTH1, are significantly up-regulated or down-regulated in CIN, accompanied by intracellular iron overload and lipid peroxidation, inducing ferroptosis. Interestingly, only TFRC expression was reversed after TMP pretreatment, as confirmed using subsequent siRNA and overexpression experiments (Figure 4). TFRC is a transmembrane glycoprotein that interacts with transferrin to mediate iron uptake. Fe^{3+} is taken up by transferrin and TFRC, reduced to Fe^{2+} , and translocated to the cytoplasmic labile iron pool via molecules such as DMT1, whereas excess Fe^{2+} is translocated by FPN [33]. However, in the presence of excess Fe^{2+} , ferroptosis can be induced by increasing intracellular ROS levels and lipid peroxidation via the Fenton reaction [34]. Cells with TFRC knockdown are more resistant to cell death induced by the ferroptosis activator erastin [35]. Recent studies have revealed that TFRC accumulation on the cell surface is a characteristic feature of ferroptosis, and ferroptosis can be distinguished from apoptosis using anti-TFRC antibodies [36]. TFRC has been shown to be up-regulated in multiple AKI models induced by nephrotoxic drugs or toxins [26,28–38]. Therefore, the TFRC may be a crucial target of TMP for regulating ferroptosis in CIN.

The characteristics of ferroptosis are depletion of glutathione and decreased activity of glutathione peroxidase 4 (GPX4). Therefore, GPX4 is considered as one of the core regulators of ferroptosis [39]. In our present study, we thus explore the changes of GPX4 in both *in vivo* and *in vitro* models. Just as shown in Figures 1 and 3, CM exposure in rats and HK-2 cells, should induce obviously decreases in GPX4 protein levels, while TMP pretreatment could significantly reverse such a decrease. These findings of ours further confirm that TMP does have a significant regulatory effect on ferroptosis in CIN.

Of course, there are still some questions that need to be further answered by future work. For example, when multiple cell death modes coexist in CIN, it is necessary to clarify the conditions for the occurrence of iron deficiency anemia and whether there is cross-talk between these mechanisms. In conclusion, TFRC-mediated ferroptosis plays a crucial role in the CIN cell model, whereas antioxidant TMP could exert an anti-ferroptosis effect to prevent such a pathological process by inhibiting TFRC and intracellular ROS production. Therefore, TMP is a promising therapeutic compound for preventing CIN.

Clinical perspectives

- Increasing evidence support the concept that ferroptosis contributes to AKI, and our previous studies indicated TMP prevent contrast medium-induced AKI (CI-AKI or CIN) *in vivo*, but whether ferroptosis is involved in TMP nephroprotective mechanism against CIN is unclear.
- Based on the data from siRNA knockdown and plasmid overexpression of TFRC, as well as classic inhibitors of ferroptosis, our present study indicates that TFRC-mediated ferroptosis plays a crucial role in CIN, whereas antioxidant TMP could exert an anti-ferroptosis effect to prevent such a pathological process by inhibiting TFRC and intracellular ROS production.
- Inhibition of the ferroptosis process in AKI is important for alleviating renal injury, our findings provide crucial insights about the potential of TMP in clinical treating AKI associated with ferroptosis.

Data Availability

All data generated or analyzed during this study are included in this article. Further enquiries can be directed to the corresponding author.

Competing Interests

The authors declare that there are no competing interests associated with the manuscript.

Funding

This study was supported by National Natural Science Foundation of China [grant numbers 82074387 and 81873280]; Shanghai Municipal Science and Technology Commission Project [grant number 20Y21902200]; and Shanghai Municipal Health Commission [grant number ZY (2021–2023)–0207–01].

CRedit Author Contribution

Zhongqiang Zhu: Software, Formal analysis, Investigation, Writing—original draft. **Jun Li:** Formal analysis, Visualization, Writing—original draft. **Zhiyong Song:** Investigation, Visualization. **Tonglu Li:** Software, Investigation. **Zongping Li:** Validation, Investigation. **Xuezhong Gong:** Conceptualization, Supervision, Methodology, Writing—review & editing.

Acknowledgements

The authors thank Prof. Zhigang Zhang of the Electron Microscopy Laboratory of Fudan University for his support in electron microscopy examination.

Abbreviations

ACSL4, acyl-CoA synthetase long-chain family; AKI, acute kidney injury; CI-AKI, contrast medium-induced AKI; CIN, contrast-induced nephropathy; DMT1, divalent metal transporter 1; FPN1, ferroportin 1; GPX4, glutathione peroxidase 4; HE, hematoxylin–eosin; HSBP1, heat shock factor binding protein 1; IHC, immunohistochemical; IREB2, iron-responsive element binding protein 2; IRI, ischemia–reperfusion injury; ROS, reactive oxygen species; TFRC, transferrin receptor.

References

- 1 Thomas, M.E., Blaine, C., Dawney, A., Devonald, M.A., Ftouh, S., Laing, C. et al. (2015) The definition of acute kidney injury and its use in practice. *Kidney Int.* **87**, 62–73, <https://doi.org/10.1038/ki.2014.328>
- 2 Hoste, E.A., Bagshaw, S.M., Bellomo, R., Cely, C.M., Colman, R., Cruz, D.N. et al. (2015) Epidemiology of acute kidney injury in critically ill patients: the multinational AKI-EPI study. *Intensive Care Med.* **41**, 1411–1423, <https://doi.org/10.1007/s00134-015-3934-7>
- 3 Ronco, C., Bellomo, R. and Kellum, J.A. (2019) Acute kidney injury. *Lancet (London, England)* **394**, 1949–1964, [https://doi.org/10.1016/S0140-6736\(19\)32563-2](https://doi.org/10.1016/S0140-6736(19)32563-2)
- 4 McCullough, P.A., Choi, J.P., Feghali, G.A., Schussler, J.M., Stoler, R.M., Vallabahn, R.C. et al. (2016) Contrast-induced acute kidney injury. *J. Am. Coll. Cardiol.* **68**, 1465–1473, <https://doi.org/10.1016/j.jacc.2016.05.099>
- 5 Yang, Y., Song, M., Liu, Y., Liu, H., Sun, L., Peng, Y. et al. (2016) Renoprotective approaches and strategies in acute kidney injury. *Pharmacol. Therapeutics* **163**, 58–73, <https://doi.org/10.1016/j.pharmthera.2016.03.015>
- 6 Dixon, S.J., Lemberg, K.M., Lamprecht, M.R., Skouta, R., Zaitsev, E.M., Gleason, C.E. et al. (2012) Ferroptosis: an iron-dependent form of nonapoptotic cell death. *Cell* **149**, 1060–1072, <https://doi.org/10.1016/j.cell.2012.03.042>
- 7 Liang, D., Minikes, A.M. and Jiang, X. (2022) Ferroptosis at the intersection of lipid metabolism and cellular signaling. *Mol. Cell.* **82**, 2215–2227, <https://doi.org/10.1016/j.molcel.2022.03.022>
- 8 Linkermann, A., Skouta, R., Himmerkus, N., Mulay, S.R., Dewitz, C., De Zen, F. et al. (2014) Synchronized renal tubular cell death involves ferroptosis. *PNAS* **111**, 16836–16841, <https://doi.org/10.1073/pnas.1415518111>
- 9 Wang, Y., Zhang, M., Bi, R., Su, Y., Quan, F., Lin, Y. et al. (2022) ACSL4 deficiency confers protection against ferroptosis-mediated acute kidney injury. *Redox Biol.* **51**, 102262, <https://doi.org/10.1016/j.redox.2022.102262>
- 10 Wang, Y., Quan, F., Cao, Q., Lin, Y., Yue, C., Bi, R. et al. (2021) Quercetin alleviates acute kidney injury by inhibiting ferroptosis. *J. Adv. Res.* **28**, 231–243, <https://doi.org/10.1016/j.jare.2020.07.007>
- 11 Guo, J., Wang, R. and Min, F. (2022) Ginsenoside Rg1 ameliorates sepsis-induced acute kidney injury by inhibiting ferroptosis in renal tubular epithelial cells. *J. Leukoc. Biol.* **112**, 1065–1077, <https://doi.org/10.1002/JLB.1A0422-211R>
- 12 Li, J. and Gong, X. (2022) Tetramethylpyrazine: an active ingredient of chinese herbal medicine with therapeutic potential in acute kidney injury and renal fibrosis. *Front. Pharmacol.* **13**, 820071, <https://doi.org/10.3389/fphar.2022.820071>
- 13 Gong, X., Wang, Q., Tang, X., Wang, Y., Fu, D., Lu, H. et al. (2013) Tetramethylpyrazine prevents contrast-induced nephropathy by inhibiting p38 MAPK and FoxO1 signaling pathways. *Am. J. Nephrol.* **37**, 199–207, <https://doi.org/10.1159/000347033>
- 14 Gong, X., Duan, Y., Zheng, J., Ye, Z. and Hei, T.K. (2019) Tetramethylpyrazine prevents contrast-induced nephropathy via modulating tubular cell mitophagy and suppressing mitochondrial fragmentation, CCL2/CCR2-mediated inflammation, and intestinal injury. *Oxidative Med. Cell. Longevity* **2019**, 7096912, <https://doi.org/10.1155/2019/7096912>
- 15 Lin, Q., Li, S., Jiang, N., Jin, H., Shao, X., Zhu, X. et al. (2021) Inhibiting NLRP3 inflammasome attenuates apoptosis in contrast-induced acute kidney injury through the upregulation of HIF1A and BNIP3-mediated mitophagy. *Autophagy* **17**, 2975–2990, <https://doi.org/10.1080/15548627.2020.1848971>

- 16 Gong, X., Ivanov, V.N., Davidson, M.M. and Hei, T.K. (2015) Tetramethylpyrazine (TMP) protects against sodium arsenite-induced nephrotoxicity by suppressing ROS production, mitochondrial dysfunction, pro-inflammatory signaling pathways and programmed cell death. *Arch. Toxicol.* **89**, 1057–1070, <https://doi.org/10.1007/s00204-014-1302-y>
- 17 Gong, X., Celsi, G., Carlsson, K., Norgren, S. and Chen, M. (2010) N-acetylcysteine amide protects renal proximal tubular epithelial cells against iohexol-induced apoptosis by blocking p38 MAPK and iNOS signaling. *Am. J. Nephrol.* **31**, 178–188, <https://doi.org/10.1159/000268161>
- 18 Kusirisin, P., Chattipakorn, S.C. and Chattipakorn, N. (2020) Contrast-induced nephropathy and oxidative stress: mechanistic insights for better interventional approaches. *J. Transl. Med.* **18**, 400, <https://doi.org/10.1186/s12967-020-02574-8>
- 19 Gong, X., Duan, Y., Zheng, J., Wang, Y., Wang, G., Norgren, S. et al. (2016) Nephroprotective effects of N-acetylcysteine amide against contrast-induced nephropathy through upregulating thioredoxin-1, inhibiting ASK1/p38MAPK pathway, and suppressing oxidative stress and apoptosis in rats. *Oxidative Med. Cell. Longevity* **2016**, 8715185, <https://doi.org/10.1155/2016/8715185>
- 20 Chen, C., Wang, D., Yu, Y., Zhao, T., Min, N., Wu, Y. et al. (2021) Legumain promotes tubular ferroptosis by facilitating chaperone-mediated autophagy of GPX4 in AKI. *Cell Death Dis.* **12**, 65, <https://doi.org/10.1038/s41419-020-03362-4>
- 21 Scarpellini, C., Klejborowska, G., Lanthier, C., Hassannia, B., Vanden Berghe, T. and Augustyns, K. (2023) Beyond ferrostatin-1: a comprehensive review of ferroptosis inhibitors. *Trends Pharmacol. Sci.* **44**, 902–916, <https://doi.org/10.1016/j.tips.2023.08.012>
- 22 Park, W., Wei, S., Kim, B.S., Kim, B., Bae, S.J., Chae, Y.C. et al. (2023) Diversity and complexity of cell death: a historical review. *Exp. Mol. Med.* **55**, 1573–1594, <https://doi.org/10.1038/s12276-023-01078-x>
- 23 Deng, F., Sharma, I., Dai, Y., Yang, M. and Kanwar, Y.S. (2019) Myo-inositol oxygenase expression profile modulates pathogenic ferroptosis in the renal proximal tubule. *J. Clin. Invest.* **129**, 5033–5049, <https://doi.org/10.1172/JCI129903>
- 24 Martín-Sánchez, D., Ruiz-Andrés, O., Poveda, J., Carrasco, S., Cannata-Ortiz, P., Sánchez-Niño, M.D. et al. (2017) Ferroptosis, but not necroptosis, is important in nephrotoxic folic acid-induced AKI. *J. Am. Soc. Nephrol.: JASN* **28**, 218–229, <https://doi.org/10.1681/ASN.2015121376>
- 25 Skouta, R., Dixon, S.J., Wang, J., Dunn, D.E., Orman, M., Shimada, K. et al. (2014) Ferrostatins inhibit oxidative lipid damage and cell death in diverse disease models. *J. Am. Chem. Soc.* **136**, 4551–4556, <https://doi.org/10.1021/ja411006a>
- 26 Hou, Y., Wang, S., Jiang, L., Sun, X., Li, J., Wang, N. et al. (2022) Patulin induces acute kidney injury in mice through autophagy-ferroptosis pathway. *J. Agric. Food Chem.* **70**, 6213–6223, <https://doi.org/10.1021/acs.jafc.1c08349>
- 27 Wang, B., Ni, Q., Wang, X. and Lin, L. (2012) Meta-analysis of the clinical effect of ligustrazine on diabetic nephropathy. *Am. J. Chin. Med.* **40**, 25–37, <https://doi.org/10.1142/S0192415X12500036>
- 28 Michel, H.E. and Menze, E.T. (2019) Tetramethylpyrazine guards against cisplatin-induced nephrotoxicity in rats through inhibiting HMGB1/TLR4/NF- κ B and activating Nrf2 and PPAR- γ signaling pathways. *Eur. J. Pharmacol.* **857**, 172422, <https://doi.org/10.1016/j.ejphar.2019.172422>
- 29 Jiang, G., Xin, R., Yuan, W., Zhang, L., Meng, X., Sun, W. et al. (2020) Ligustrazine ameliorates acute kidney injury through downregulation of NOD2-mediated inflammation. *Int. J. Mol. Med.* **45**, 731–742, <https://doi.org/10.3892/ijmm.2020.4464>
- 30 Sun, W., Li, A., Wang, Z., Sun, X., Dong, M., Qi, F. et al. (2020) Tetramethylpyrazine alleviates acute kidney injury by inhibiting NLRP3/HIF-1 α and apoptosis. *Mol. Med. Reports* **22**, 2655–2664, <https://doi.org/10.3892/mmr.2020.11378>
- 31 Ying, J., Wu, J., Zhang, Y., Han, Y., Qian, X., Yang, Q. et al. (2020) Ligustrazine suppresses renal NMDAR1 and caspase-3 expressions in a mouse model of sepsis-associated acute kidney injury. *Mol. Cell. Biochem.* **464**, 73–81, <https://doi.org/10.1007/s11010-019-03650-4>
- 32 Sureshbabu, A., Ryter, S.W. and Choi, M.E. (2015) Oxidative stress and autophagy: crucial modulators of kidney injury. *Redox Biol.* **4**, 208–214, <https://doi.org/10.1016/j.redox.2015.01.001>
- 33 Gammella, E., Buratti, P., Cairo, G. and Recalcati, S. (2017) The transferrin receptor: the cellular iron gate. *Metallomics: Integrated Biometal Sci.* **9**, 1367–1375, <https://doi.org/10.1039/C7MT00143F>
- 34 Jiang, X., Stockwell, B.R. and Conrad, M. (2021) Ferroptosis: mechanisms, biology and role in disease. *Nat. Rev. Mol. Cell Biol.* **22**, 266–282, <https://doi.org/10.1038/s41580-020-00324-8>
- 35 Yang, W.S. and Stockwell, B.R. (2008) Synthetic lethal screening identifies compounds activating iron-dependent, nonapoptotic cell death in oncogenic-RAS-harboring cancer cells. *Chemistry Biol.* **15**, 234–245, <https://doi.org/10.1016/j.chembiol.2008.02.010>
- 36 Feng, H., Schorpp, K., Jin, J., Yozwiak, C.E., Hoffstrom, B.G., Decker, A.M. et al. (2020) Transferrin receptor is a specific ferroptosis marker. *Cell Rep.* **30**, 3411.e7–3423.e7, <https://doi.org/10.1016/j.celrep.2020.02.049>
- 37 Ikeda, Y., Hamano, H., Horinouchi, Y., Miyamoto, L., Hirayama, T., Nagasawa, H. et al. (2021) Role of ferroptosis in cisplatin-induced acute nephrotoxicity in mice. *J. Trace Elements Med. Biol.: Organ Soc. Minerals Trace Elements (GMS)* **67**, 126798, <https://doi.org/10.1016/j.jtemb.2021.126798>
- 38 Li, H., Wang, B., Wu, S., Dong, S., Jiang, G., Huang, Y. et al. (2023) Ferroptosis is involved in polymyxin B-induced acute kidney injury via activation of p53. *Chem. Biol. Interact.* **378**, 110479, <https://doi.org/10.1016/j.cbi.2023.110479>
- 39 Liu, S., Zhao, X., Shui, S., Wang, B., Cui, Y., Dong, S. et al. (2022) PDTAC: targeted photodegradation of GPX4 triggers ferroptosis and potent antitumor immunity. *J. Med. Chem.* **65**, 12176–12187, <https://doi.org/10.1021/acs.jmedchem.2c00855>